

The Woodpecker Toy

Christoph Glocker and Christian Studer
IMES - Center for Mechanics
ETH Zürich, Switzerland

June 5, 2003

1 Introduction

The aim of this paper is twofold: On the one hand, we want to present a theoretical framework that is sufficiently wide to treat fully finite-dimensional dynamic systems with planar unilateral Coulomb-contact constraints. An example that fits in with this class of problems is the woodpecker toy, which might serve as one of the benchmark problems in the SICONOS project. Our second goal is to show a general strategy on how to set up linear complementarity problems in a most efficient way when set-valued relay functions are involved. This step is non-trivial. In our approach, an LCP in standard form is generated with closest possible connection to optimization theory and with a minimum of equations and operations for matrix inversion.

A woodpecker hammering down a pole is a typical low-dimensional system combining unilateral constraints, impacts, Coulomb friction and jamming. The woodpecker toy (figure 1) consists of a pole, a sleeve with a hole that is slightly larger than the diameter of the pole, a spring, and the woodpecker. In operation, the woodpecker moves downwards the pole performing some kind of pitching motion, which is controlled by the sleeve. This mechanism of self-excitation may roughly be explained as follows: Gravitation acts as an energy source. This energy is transmitted to the woodpecker and results in a vertical downwards motion of the entire system. The woodpecker itself oscillates up and down. This oscillation interacts via the spring with the sleeve. It gains its energy from the downwards motion by turning the sleeve and switching on and off a frictional contact jamming of the sleeve at the pole. This mechanism ends up in a stable limit cycle with an energetic balance of the kinetic energy gained per cycle by the falling height and the dissipated energy due to the frictional contacts.

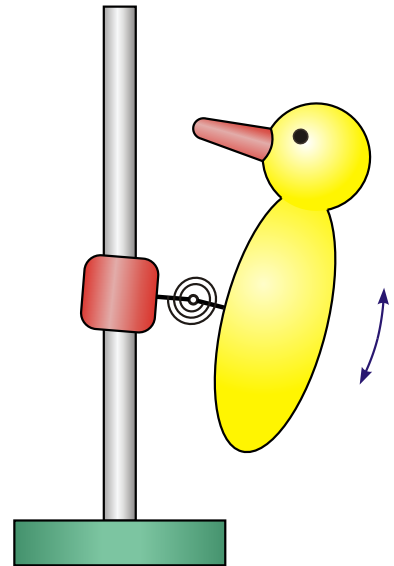


Figure 1: Woodpecker Toy

The paper is organized as follows: In section 2 we introduce the two most basic set-valued maps defined on \mathbb{R} , the unilateral primitive $\text{Upr}(x)$ and the filled-in relay function $\text{Sgn}(x)$. We show that the relay function can be expressed by two unilateral primitives, which is later substantial when the LCP of the dynamic system with planar frictional contacts is formulated. The theoretical framework on how to state a frictional contact problem in finite freedom dynamics is shortly presented in section 3. We follow exactly the work in [4], but narrow it down already to planar unilateral Coulomb contacts with Newtonian impacts to have later access to linear complementarity. We give a complete formulation of the dynamic process based on a measure differential inclusion and try to clearly arrange the full set of unilateral contact-impact laws. The woodpecker in section 4 serves as a typical example for such systems. We show the full model together with a complete list of parameters that have been used for the numerical simulation. As results, we present the time history of the woodpecker's and sleeve's angular displacements and velocities, and the associated limit cycles in the phase space. Section 5 reviews the midpoint rule that was introduced in [4] to perform time discretization and that we used to numerically integrate the woodpecker's equations. In section 6 we finally show how the linear complementarity problem has to be formulated for planar Coulomb contacts by using the discretized equations of section 5. This procedure has been taken from [2] and has been adapted to fit in with impacts.

2 Basic Set-Valued Elements

A linear complementarity problem (LCP) is a problem of the form: For given $\mathbf{A} \in \mathbb{R}^{n,n}$ and $\mathbf{b} \in \mathbb{R}^n$, find $\mathbf{x} \in \mathbb{R}^n$ and $\mathbf{y} \in \mathbb{R}^n$ such that the linear equation $\mathbf{y} = \mathbf{Ax} + \mathbf{b}$ holds together with the complementarity conditions $y_i \geq 0$, $x_i \geq 0$, $y_i x_i = 0$ for $i = 1, \dots, n$. The latter are often written in the form $\mathbf{y} \geq 0$, $\mathbf{x} \geq 0$, $\mathbf{y}^\top \mathbf{x} = 0$ or, equivalently, as $0 \leq \mathbf{y} \perp \mathbf{x} \geq 0$.

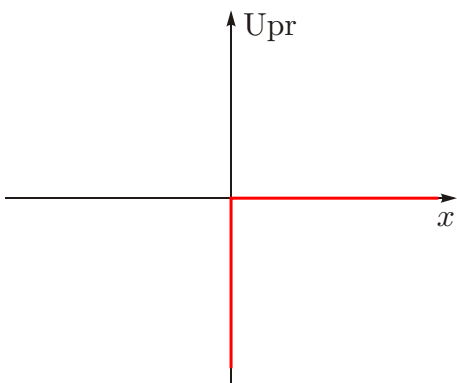


Figure 2: The map $x \rightarrow \text{Upr}(x)$

It is convenient to introduce a maximal monotone set-valued map Upr defined on \mathbb{R}^+ , which we call the *unilateral primitive* [1],

$$\text{Upr}(x) := \begin{cases} \{0\} & \text{if } x > 0 \\ [-\infty, 0] & \text{if } x = 0 \end{cases}. \quad (1)$$

The graph of this map is depicted in figure 2. Apparently, we are now able to express each complementarity condition of the LCP by one inclusion,

$$-y \in \text{Upr}(x) \Leftrightarrow y \geq 0, x \geq 0, xy = 0. \quad (2)$$

Unilateral primitives are used in mechanics on displacement and on velocity level to model unilateral constraints and one-way clutches. The associated set-valued force laws are then stated as inclusions in the form (2).

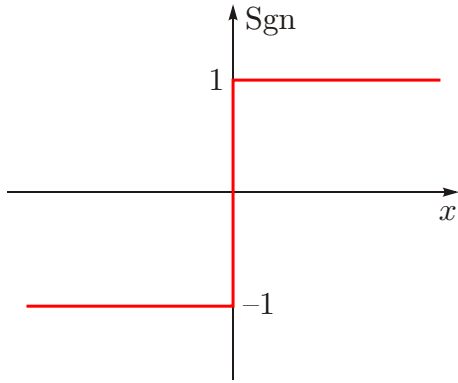


Figure 3: The map $x \rightarrow \text{Sgn}(x)$

A second maximal monotone set-valued map frequently met in complementarity systems is the filled-in *relay function* $\text{Sgn}(x)$, defined by

$$\text{Sgn}(x) := \begin{cases} \{+1\} & \text{if } x > 0 \\ [-1, +1] & \text{if } x = 0 \\ \{-1\} & \text{if } x < 0 \end{cases}, \quad (3)$$

see figure 3 for the graph. Note the difference at $x = 0$ to the classical sgn -function, which is defined as $\text{sgn}(x = 0) = 0$. In mechanics, relay functions on velocity level are used to model any kind of dry friction. On displacement level, they describe the behavior of pre-stressed springs. The relay function (3) can be represented by two unilateral primitives as indicated in figure 4, which yields in terms of inclusions

$$-y \in \text{Sgn}(x) \Leftrightarrow \exists x_R, x_L \text{ such that } \begin{cases} -y \in +\text{Upr}(x_R) + 1 \\ -y \in -\text{Upr}(x_L) - 1 \\ x = x_R - x_L \end{cases}. \quad (4)$$

More details on this decomposition may be found in [2] together with various applications of even more complex set-valued interaction laws and their representations via unilateral primitives. By using (2), we may finally express (4) in terms of complementarities,

$$-y \in \text{Sgn}(x) \Leftrightarrow \exists x_R, x_L \text{ such that } \begin{cases} 1 + y \geq 0, x_R \geq 0, (1 + y)x_R = 0 \\ 1 - y \geq 0, x_L \geq 0, (1 - y)x_L = 0 \\ x = x_R - x_L \end{cases} \quad (5)$$

This representation has to be used when a problem involving Sgn -multifunctions is formulated as an LCP in standard form.

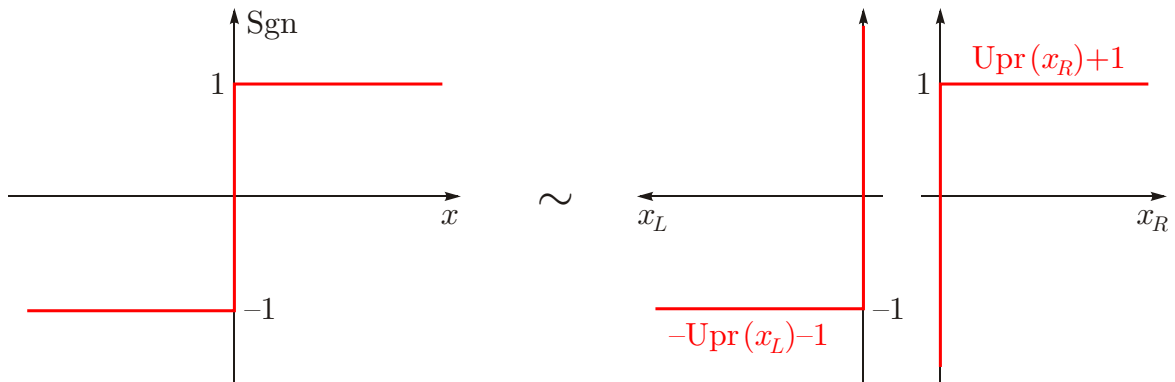


Figure 4: Decomposition of Sgn into Upr 's

3 Mechanical Systems with Planar Coulomb Friction

The most suitable way to express the Newton-Euler equations for non-smooth dynamics is in terms of an equality of measures as introduced in [4]. Beside the non-smooth impact-free motion, this formulation even covers impulsive behavior, and should be considered as the starting point of any such problem in dynamics.

The following notation is used: $I := [t_A, t_E]$ denotes a compact time interval on which the motion of the system is of interest. Time is denoted by t , and the Lebesgue measure on \mathbb{R} by dt . We investigate the dynamics of a mechanical system on an f -dimensional configuration manifold with frictional boundaries. The set of local coordinates in use is denoted by $\mathbf{q} \in \mathbb{R}^f$, and the associated velocities by $\mathbf{u} \in \mathbb{R}^f$. As functions of time, the velocities $\mathbf{u}: [t_A, t_E] \rightarrow \mathbb{R}^f$ are assumed to be of bounded variation with differential measure $d\mathbf{u}$, leading to displacements $\mathbf{q}(t) = \mathbf{q}(t_A) + \int_{t_A}^t \mathbf{u}(\tau) d\tau$ that are absolutely continuous on I with $\dot{\mathbf{q}} = \mathbf{u}$ almost everywhere. We further denote by $\mathbf{u}^+(t)$ and $\mathbf{u}^-(t)$ the right and left limit of $\mathbf{u}(t)$ at t , respectively, which might be different from each other in the case of an impact. The measure equality for such a system reads

$$\mathbf{M} d\mathbf{u} - \mathbf{h} dt - d\mathbf{R} = 0, \quad (6)$$

where $\mathbf{M}(\mathbf{q}, t)$ is the symmetric and positive definite mass matrix of the system, $\mathbf{h}(\mathbf{q}, \mathbf{u}, t)$ the f -tuple of the gyroscopical accelerations (Christoffel symbols) together with all classical finite-valued generalized forces, and $d\mathbf{R}$ the force measure of possibly atomic impact impulsions, in our case containing the contact forces. The terms \mathbf{M} and \mathbf{h} can be derived, for example, by taking \mathbf{q} as a set of classical generalized coordinates of the system and evaluating Lagrange's equations of second kind or the associated virtual work expressions. The resulting classical second order equation $\mathbf{M}(\mathbf{q}, t) \ddot{\mathbf{q}} - \mathbf{h}(\mathbf{q}, \dot{\mathbf{q}}, t) = 0$ would then describe the same system as above, but without any contacts and any contact forces.

We assume a total of n frictional unilateral constraints in the system, which are represented by n inequalities

$$g_{Ni}(\mathbf{q}, t) \geq 0, \quad i = 1, \dots, n \quad (7)$$

The g_{Ni} are the gap functions of the frictional contacts. They are formulated such that $g_{Ni} > 0$ indicates an open contact with an Euclidean distance of the contact points given by the value of g_{Ni} , $g_{Ni} = 0$ corresponds to a closed contact, and $g_{Ni} < 0$ indicates forbidden overlapping or interpenetration. A detailed description on how to define these inequalities in a multibody system may be found in [5]. We further introduce the set of active contacts

$$\mathcal{H}(t) = \{ i \mid g_{Ni}(\mathbf{q}(t), t) = 0 \} \quad (8)$$

which singles out the contacts at which contact forces may occur. The force measure $d\mathbf{R}$ in (6) is therefore at most composed of the normal and tangential contact forces of the individuals $i \in \mathcal{H}$ and may be written as

$$d\mathbf{R} = \sum_{i \in \mathcal{H}} \mathbf{w}_{Ni} d\Lambda_{Ni} + \mathbf{w}_{Ti} d\Lambda_{Ti}. \quad (9)$$

In this expression, $(\mathbf{w}_{Ni}, \mathbf{w}_{Ti})$ are the generalized normal and tangential force directions, and $(d\Lambda_{Ni}, d\Lambda_{Ti})$ the scalar normal and tangential contact impulse measure of contact i . Note that integration over a singleton t gives the scalar impulsive contact forces, $\int_{\{t\}}(d\Lambda_{Ni}, d\Lambda_{Ti}) = (\Lambda_{Ni}(t), \Lambda_{Ti}(t))$, whereas $(d\Lambda_{Ni}, d\Lambda_{Ti}) = (A'_{Ni}, A'_{Ti}) dt$ for impact-free motion with A'_{Ni} the normal and A'_{Ti} the tangential scalar contact force.

The system's dynamics is not yet completely determined by equations (6)–(9), because we have still to specify force laws that express the contact impulse measures $(d\Lambda_{Ni}, d\Lambda_{Ti})$ in terms of the system's kinematic state (\mathbf{q}, \mathbf{u}) . To do so, we introduce first the normal and tangential relative velocities in the contacts,

$$\gamma_{Ni} = \mathbf{w}_{Ni}^\top \mathbf{u} + \hat{w}_{Ni}, \quad \gamma_{Ti} = \mathbf{w}_{Ti}^\top \mathbf{u} + \hat{w}_{Ti} \quad (10)$$

with $(\mathbf{w}_{Ni}, \mathbf{w}_{Ti})(\mathbf{q}, t)$ as in (9) and $(\hat{w}_{Ni}, \hat{w}_{Ti})(\mathbf{q}, t) \neq (0, 0)$ only for rheonomic systems, see e.g. [5] on how to obtain these terms. We choose for the normal direction of each contact a unilateral version of Newton's impact law with local restitution coefficient $\varepsilon_{Ni} \in [0, 1]$, and for the tangential direction a Coulomb type frictional law with friction coefficient μ_i that is complemented by tangential restitution behavior $\varepsilon_{Ti} \in [0, 1]$. We define

$$\xi_{Ni} := \gamma_{Ni}^+ + \varepsilon_{Ni} \gamma_{Ni}^-, \quad \xi_{Ti} := \gamma_{Ti}^+ + \varepsilon_{Ti} \gamma_{Ti}^-, \quad (11)$$

where $(\gamma_{Ni}^\pm, \gamma_{Ti}^\pm) := (\gamma_{Ni}, \gamma_{Ti})(\mathbf{u}^\pm)$, and pose the normal and tangential impact laws as

$$-d\Lambda_{Ni} \in \text{Upr}(\xi_{Ni}), \quad -d\Lambda_{Ti} \in \mu_i d\Lambda_{Ni} \text{Sgn}(\xi_{Ti}). \quad (12)$$

With equations (6)–(12) we have now obtained a complete description of the dynamics of the system, including both, impacts and impact-free motion.

Note that the impact laws (12) are actually impact-contact laws, because they hold for both, impacts and impact-free motion: In the first case, $(d\Lambda_{Ni}, d\Lambda_{Ti})$ in (12) has just to be replaced by the corresponding impulses $(\Lambda_{Ni}, \Lambda_{Ti})(t)$ when integration over $\{t\}$ has been performed. For the second case, assume a time interval without impacts, i.e. a time interval in which $\mathbf{u}^+ = \mathbf{u}^- = \mathbf{u}$ and $(d\Lambda_{Ni}, d\Lambda_{Ti}) = (A'_{Ni}, A'_{Ti}) dt$. Under these assumptions, (11) becomes

$$\xi_{Ni} = (1 + \varepsilon_{Ni}) \gamma_{Ni}, \quad \xi_{Ti} = (1 + \varepsilon_{Ti}) \gamma_{Ti},$$

which causes (12) to be

$$-A'_{Ni} dt \in \text{Upr}((1 + \varepsilon_{Ni}) \gamma_{Ni}), \quad -A'_{Ti} dt \in \mu_i A'_{Ni} dt \text{Sgn}((1 + \varepsilon_{Ti}) \gamma_{Ti}).$$

With $(\varepsilon_{Ni} \geq 0, \varepsilon_{Ti} \geq 0)$ and after “crossing out” dt from both inclusions, one obtains

$$-A'_{Ni} \in \text{Upr}(\gamma_{Ni}), \quad -A'_{Ti} \in \mu_i A'_{Ni} \text{Sgn}(\gamma_{Ti}),$$

which are the force laws for impact-free motion of unilaterally constrained contacts with Coulomb friction [5].

4 The Woodpecker

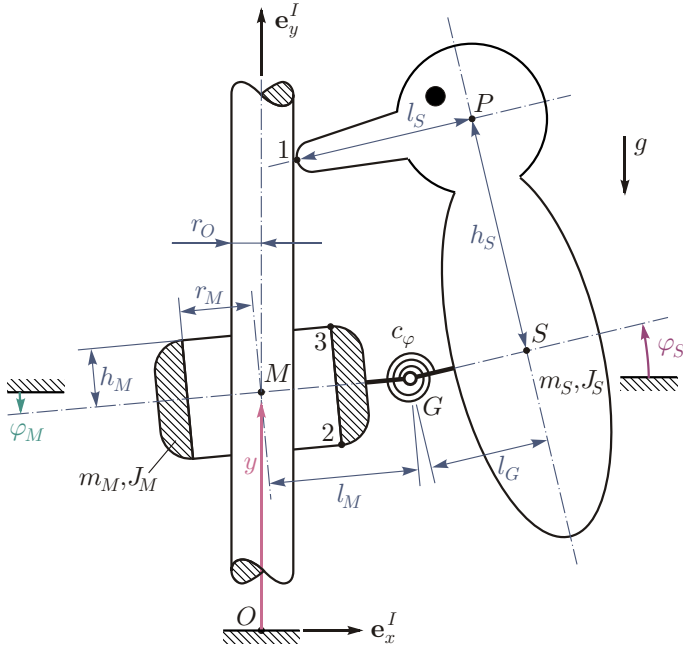


Figure 5: Mechanical model of the woodpecker

A planar model of the woodpecker toy is shown in figure 5. It consists of three rigid bodies: The woodpecker (center of mass S , mass m_S , moment of inertia J_S), the sleeve (center of mass M , mass m_M , moment of inertia J_M), and the pole that is fixed to the environment. The woodpecker and the sleeve are connected by a revolute joint with angular stiffness c_φ and are both under the influence of gravity g . We equipped the system with three degrees of freedom that are the angular displacement φ_S of the woodpecker, and the angular and vertical displacements φ_M and y of the sleeve. Lateral deviations of the sleeve are small and thus not considered in the model. We further

denote the angular velocity of the woodpecker by ω_S , and the angular and vertical velocities of the sleeve by ω_M and v . The generalized coordinates \mathbf{q} and associated velocities \mathbf{u} may thus be chosen as

$$\mathbf{q} = \begin{pmatrix} y \\ \varphi_M \\ \varphi_S \end{pmatrix}, \quad \mathbf{u} = \begin{pmatrix} v \\ \omega_M \\ \omega_S \end{pmatrix} \quad \text{with } \dot{\mathbf{q}} = \mathbf{u} \text{ almost everywhere.} \quad (13)$$

The special geometrical design of the toy led us to assume only small deviations in the displacements during operation. Thus we set up the dynamic equations (6)–(10) based on a linearized kinematics. The mass matrix \mathbf{M} and the vector \mathbf{h} in (6)

$$\mathbf{M} = \begin{pmatrix} m_S + m_M & m_S l_M & m_S l_G \\ m_S l_M & J_M + m_S l_M^2 & m_S l_M l_G \\ m_S l_G & m_S l_M l_G & J_S + m_S l_G^2 \end{pmatrix} \quad \mathbf{h} = \begin{pmatrix} -(m_S + m_M)g \\ -c_\varphi(\varphi_M - \varphi_S) - m_S l_M g \\ -c_\varphi(\varphi_S - \varphi_M) - m_S l_G g \end{pmatrix} \quad (14)$$

follow in a straightforward manner from the kinetic and potential energy of the system by working out Lagrange's equations of second kind.

Altogether we took into account three different frictional contacts: Contact 1 is between the beak of the woodpecker and the pole. This contact constraint is not necessary for the woodpecker to work, but as beak impacts have been observed in reality, we wanted them to be included in our model. The more important contacts are between the sleeve and the pole: The diameter of the hole in the sleeve is slightly larger than the diameter

of the pole. Due to the resulting clearance, the lower or upper edge of the sleeve may come into contact with the pole. This is modeled by the unilateral constraints 2 and 3. In particular, the lower sleeve contact 2 is most essential for the jamming mechanism to be switched on and off. The three gap functions (7) follow now directly from figure 5,

$$\begin{aligned} g_{N1} &= (l_M + l_G - l_S - r_O) - h_S \varphi_S, \\ g_{N2} &= (r_M - r_O) + h_M \varphi_M, \\ g_{N3} &= (r_M - r_O) - h_M \varphi_M. \end{aligned} \tag{15}$$

The relative velocities (10) in the normal directions γ_{Ni} are directly obtained by differentiating the gap functions (15) with respect to time. In the tangential directions, the γ_{Ti} follow easily from figure 5. The associated \mathbf{w} vectors and \hat{w} scalars that are also needed to set up the force measure $d\mathbf{R}$ in (9) are

$$\begin{aligned} \mathbf{w}_{N1} &= \begin{pmatrix} 0 \\ 0 \\ -h_S \end{pmatrix}, \quad \mathbf{w}_{T1} = \begin{pmatrix} 1 \\ l_M \\ l_G - l_S \end{pmatrix}, \quad \hat{w}_{N1} = \hat{w}_{T1} = 0, \\ \mathbf{w}_{N2} &= \begin{pmatrix} 0 \\ h_M \\ 0 \end{pmatrix}, \quad \mathbf{w}_{T2} = \begin{pmatrix} 1 \\ r_M \\ 0 \end{pmatrix}, \quad \hat{w}_{N2} = \hat{w}_{T2} = 0, \\ \mathbf{w}_{N3} &= \begin{pmatrix} 0 \\ -h_M \\ 0 \end{pmatrix}, \quad \mathbf{w}_{T3} = \begin{pmatrix} 1 \\ r_M \\ 0 \end{pmatrix}, \quad \hat{w}_{N3} = \hat{w}_{T3} = 0. \end{aligned} \tag{16}$$

Numerical integration of the system has been performed by applying the time stepping method described in the next section. The parameters used together with the initial conditions are summarized in table 1. The results in figures 6–8 obtained by this method have been confirmed by an event-driven evaluation of the same system which is published in [3], complemented by a deep discussion of the bifurcation behavior of the system.

geometry	radius of pole	$r_O = 0.0025$ m
	inner radius of sleeve	$r_M = 0.0031$ m
	$\frac{1}{2}$ height of sleeve	$h_M = 0.0058$ m
	distance M – G	$l_M = 0.010$ m
	distance G – S	$l_G = 0.015$ m
	distance S – P	$h_S = 0.02$ m
	length of beak P –1	$l_S = 0.0201$ m
inertias	mass, sleeve	$m_M = 0.0003$ kg
	mass, woodpecker	$m_S = 0.0045$ kg
	moment of inertia, sleeve	$J_M = 5.0 \cdot 10^{-9}$ kg m ²
	moment of inertia, woodpecker	$J_S = 7.0 \cdot 10^{-7}$ kg m ²

force elements	angular stiffness, spring	$c_\varphi = 0.0056 \frac{\text{Nm}}{\text{rad}}$
	gravity	$g = 9.81 \frac{\text{m}}{\text{s}^2}$
contact parameters	normal restitution	$\varepsilon_{N1} = 0.5$
		$\varepsilon_{N2,3} = 0$
	tangential restitution	$\varepsilon_{T1,2,3} = 0$
	friction coefficients	$\mu_{1,2,3} = 0.3$
initial conditions	sleeve, displacement	$y(0) = 0 \text{ m}$
	sleeve, angle	$\varphi_M(0) = -0.1036 \text{ rad}$
	woodpecker, angle	$\varphi_S(0) = -0.2788 \text{ rad}$
	sleeve, velocity	$v(0) = -0.3411 \frac{\text{m}}{\text{s}}$
	sleeve, angular velocity	$\omega_M(0) = 0 \frac{\text{rad}}{\text{s}}$
	woodpecker, angular velocity	$\omega_S(0) = -7.4583 \frac{\text{rad}}{\text{s}}$

Table 1: Parameters and initial conditions

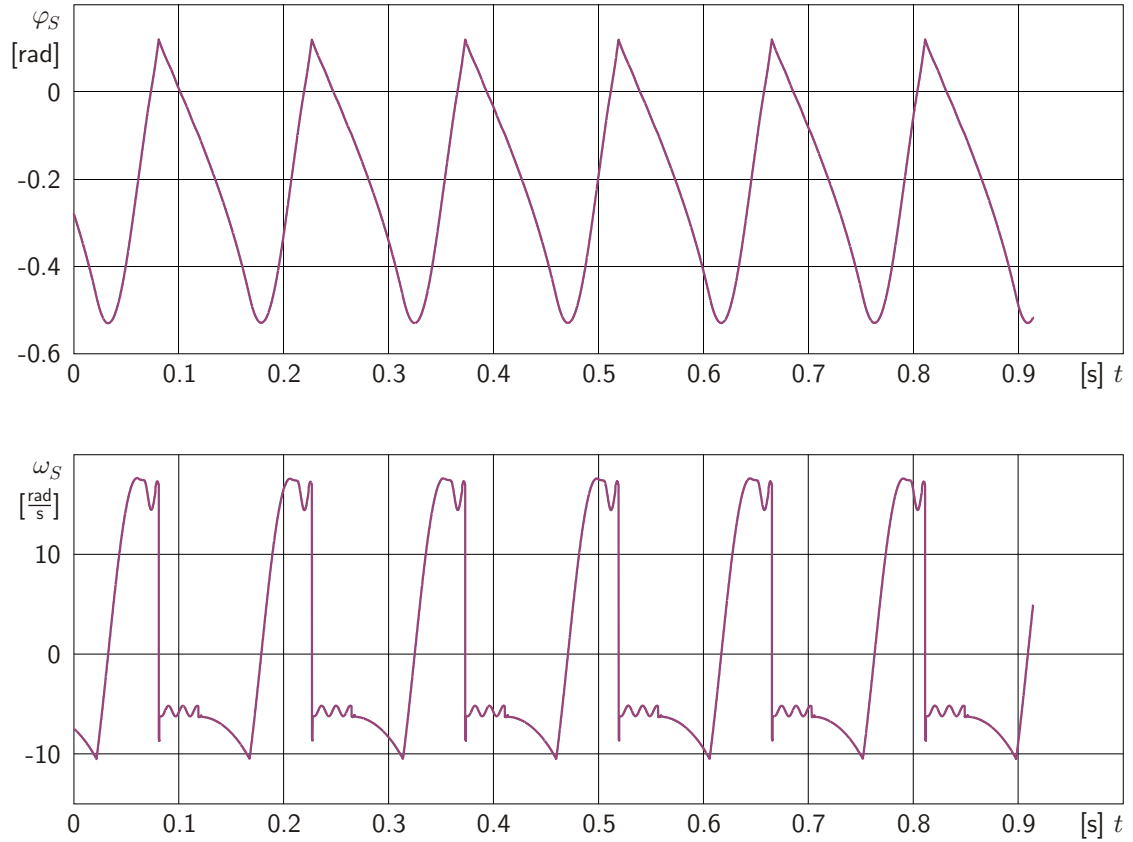


Figure 6: Time history of the woodpecker's angular displacement and velocity.

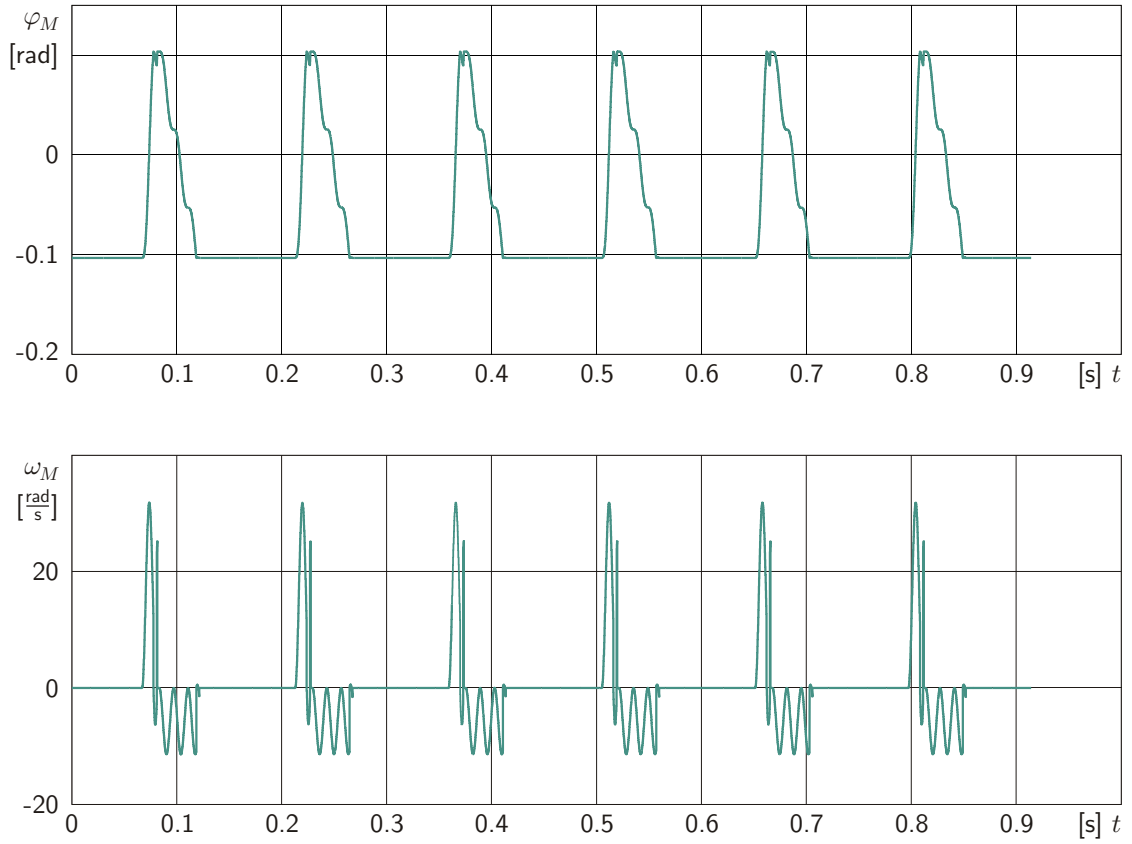


Figure 7: Time history of the sleeve's angular displacement and velocity.

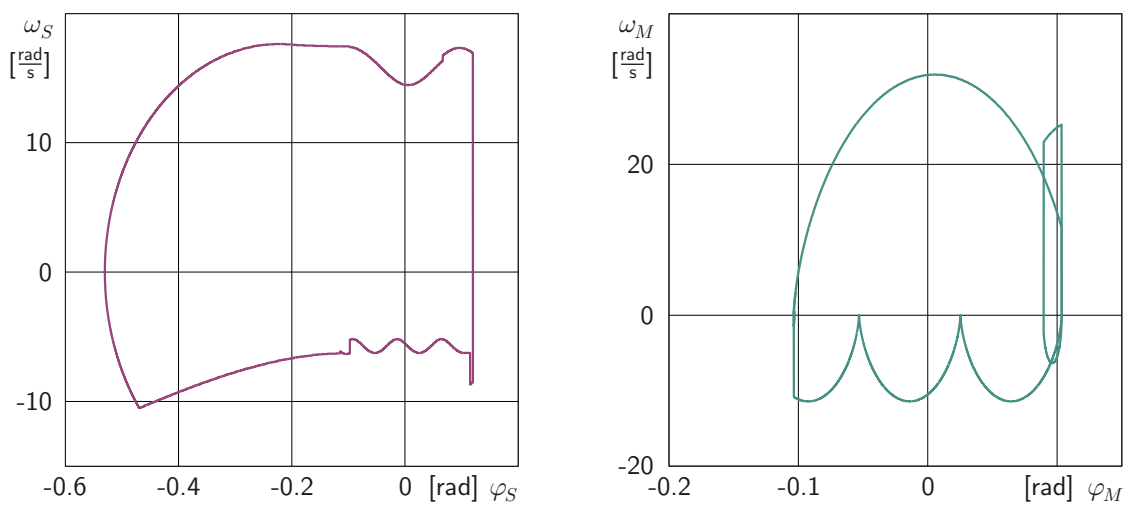


Figure 8: Limit cycle in the phase space.

5 Time Discretization

In this section we review the midpoint rule presented in [4] to perform the numerical integration of the system (6)–(12). We may pose the problem as follows: For given initial time t^A and known initial displacements $\mathbf{q}^A := \mathbf{q}(t^A) \in \mathbb{R}^f$ and velocities $\mathbf{u}^A := \mathbf{u}(t^A) \in \mathbb{R}^f$, find the displacements $\mathbf{q}^E := \mathbf{q}(t^E) \in \mathbb{R}^f$ and velocities $\mathbf{u}^E := \mathbf{u}(t^E) \in \mathbb{R}^f$ at the end t^E of a chosen time interval $[t^A, t^E]$. The following steps have to be performed:

1. Choose a time step Δt and compute the midpoint $t^M := t^A + \frac{1}{2} \Delta t$ and the endpoint $t^E := t^A + \Delta t$ of the time interval
2. Compute the midpoint displacements $\mathbf{q}^M := \mathbf{q}^A + \frac{1}{2} \Delta t \cdot \mathbf{u}^A \in \mathbb{R}^f$
3. Matrix calculations:
 - (a) Compute $\mathbf{M}(\mathbf{q}^M, t^M) \in \mathbb{R}^{f,f}$ and $\mathbf{h}(\mathbf{q}^M, \mathbf{u}^A, t^M) \in \mathbb{R}^f$
 - (b) For $i = 1, \dots, n$ set up the index set $\mathcal{H} := \{i \mid g_{Ni}(\mathbf{q}^M, t^M) \leq 0\}$ with k elements i_1, \dots, i_k ($0 \leq k \leq n$)
 - (c) For every $i \in \mathcal{H}$ compute $\mathbf{w}_{Ni}(\mathbf{q}^M, t^M) \in \mathbb{R}^f$ and $\hat{w}_{Ni}(\mathbf{q}^M, t^M) \in \mathbb{R}$, as well as $\mathbf{w}_{Ti}(\mathbf{q}^M, t^M) \in \mathbb{R}^f$ and $\hat{w}_{Ti}(\mathbf{q}^M, t^M) \in \mathbb{R}$
4. Computation of \mathbf{u}^E : In this step, the equations (6), (9), (10), (11) and inclusions (12) have to be solved: Find \mathbf{u}^E such that for $i \in \mathcal{H}$

$$\begin{aligned}
(6, 9): \quad & \mathbf{M}(\mathbf{u}^E - \mathbf{u}^A) - \mathbf{h} \Delta t - \sum_{i \in \mathcal{H}} (\mathbf{w}_{Ni} \Lambda_{Ni} + \mathbf{w}_{Ti} \Lambda_{Ti}) = 0 \\
(10): \quad & \gamma_{Ni}^E = \mathbf{w}_{Ni}^\top \mathbf{u}^E + \hat{w}_{Ni} \quad \gamma_{Ti}^E = \mathbf{w}_{Ti}^\top \mathbf{u}^E + \hat{w}_{Ti} \\
(10): \quad & \gamma_{Ni}^A = \mathbf{w}_{Ni}^\top \mathbf{u}^A + \hat{w}_{Ni} \quad \gamma_{Ti}^A = \mathbf{w}_{Ti}^\top \mathbf{u}^A + \hat{w}_{Ti} \\
(11): \quad & \xi_{Ni} = \gamma_{Ni}^E + \varepsilon_{Ni} \gamma_{Ni}^A \quad \xi_{Ti} = \gamma_{Ti}^E + \varepsilon_{Ti} \gamma_{Ti}^A \\
(12): \quad & -\Lambda_{Ni} \in \text{Upr}(\xi_{Ni}) \quad -\Lambda_{Ti} \in \mu_i \Lambda_{Ni} \text{Sgn}(\xi_{Ti})
\end{aligned} \tag{17}$$

The numerical solution of this problem can be obtained by many different methods. One possibility is to formulate it as an LCP which will be done in the next section, and to invoke an appropriate LCP solver.

5. Computation of $\mathbf{q}^E := \mathbf{q}^M + \frac{1}{2} \Delta t \cdot \mathbf{u}^E \in \mathbb{R}^f$

6 Setting up the LCP

The purpose of this section is to derive an LCP formulation of the problem (17). This step is nontrivial and tricky, and *must not be underestimated!* The main difficulty stems from the Sgn-functions that have to be decomposed to achieve the desired complementarity formulation.

There are many different approaches found in the literature on how to perform this decomposition. Slack variables are introduced in various ways to express the relay function by complementarity conditions. Most of them, however, have serious disadvantages with respect to the dimension or the structure of the resulting LCP. Possible relations to optimization theory may easily be disguised when slack variables are introduced in an ad hoc manner. Other problems are that additional solutions, that means solutions that are *not* contained in the original problem and thus *contradict the original problem*, might be generated when too many slack variables are introduced without the necessary care, or that unnecessary matrix inversions have to be performed. Another attempt that is frequently undertaken and that does *not* solve the problem is to slightly shift the set-valuedness of the Sgn-function away from the origin to a neighboring point.

We are convinced that our approach is *the only reasonable* when an LCP representation in local variables is desired for systems involving relay functions, and that this approach is even general enough to be applied without any modifications for adjoint problems in electrical networks or hydraulics. The steps that we perform to derive the LCP follow exactly the procedure described in [2] to approximate even spatial friction by friction pyramides. To set up the LCP, rigorous matrix notation is required. We define

$$\begin{array}{ll}
\mathbf{W}_N := (\mathbf{w}_{Ni_1}, \dots, \mathbf{w}_{Ni_k}) & \in \mathbb{R}^{f,k} & \mathbf{W}_T := (\mathbf{w}_{Ti_1}, \dots, \mathbf{w}_{Ti_k}) & \in \mathbb{R}^{f,k} \\
\hat{\mathbf{w}}_N := (\hat{w}_{Ni_1}, \dots, \hat{w}_{Ni_k})^\top & \in \mathbb{R}^k & \hat{\mathbf{w}}_T := (\hat{w}_{Ti_1}, \dots, \hat{w}_{Ti_k})^\top & \in \mathbb{R}^k \\
\mathbf{\Lambda}_N := (\Lambda_{Ni_1}, \dots, \Lambda_{Ni_k})^\top & \in \mathbb{R}^k & \mathbf{\Lambda}_T := (\Lambda_{Ti_1}, \dots, \Lambda_{Ti_k})^\top & \in \mathbb{R}^k \\
\boldsymbol{\gamma}_N^E := (\gamma_{Ni_1}^E, \dots, \gamma_{Ni_k}^E)^\top & \in \mathbb{R}^k & \boldsymbol{\gamma}_T^E := (\gamma_{Ti_1}^E, \dots, \gamma_{Ti_k}^E)^\top & \in \mathbb{R}^k \\
\boldsymbol{\gamma}_N^A := (\gamma_{Ni_1}^A, \dots, \gamma_{Ni_k}^A)^\top & \in \mathbb{R}^k & \boldsymbol{\gamma}_T^A := (\gamma_{Ti_1}^A, \dots, \gamma_{Ti_k}^A)^\top & \in \mathbb{R}^k \\
\boldsymbol{\xi}_N := (\xi_{Ni_1}, \dots, \xi_{Ni_k})^\top & \in \mathbb{R}^k & \boldsymbol{\xi}_T := (\xi_{Ti_1}, \dots, \xi_{Ti_k})^\top & \in \mathbb{R}^k \\
\boldsymbol{\epsilon}_N := \text{diag}(\epsilon_{Ni_1}, \dots, \epsilon_{Ni_k}) & \in \mathbb{R}^{k,k} & \boldsymbol{\epsilon}_T := \text{diag}(\epsilon_{Ti_1}, \dots, \epsilon_{Ti_k}) & \in \mathbb{R}^{k,k} \\
& & \boldsymbol{\mu} := \text{diag}(\mu_{i_1}, \dots, \mu_{i_k}) & \in \mathbb{R}^{k,k}
\end{array}$$

and rewrite the first four lines in (17) as

$$\begin{array}{l}
\mathbf{M}(\mathbf{u}^E - \mathbf{u}^A) - \mathbf{h} \Delta t - \mathbf{W}_N \mathbf{\Lambda}_N - \mathbf{W}_T \mathbf{\Lambda}_T = 0 \\
\boldsymbol{\gamma}_N^E = \mathbf{W}_N^\top \mathbf{u}^E + \hat{\mathbf{w}}_N \quad \boldsymbol{\gamma}_T^E = \mathbf{W}_T^\top \mathbf{u}^E + \hat{\mathbf{w}}_T \\
\boldsymbol{\gamma}_N^A = \mathbf{W}_N^\top \mathbf{u}^A + \hat{\mathbf{w}}_N \quad \boldsymbol{\gamma}_T^A = \mathbf{W}_T^\top \mathbf{u}^A + \hat{\mathbf{w}}_T \\
\boldsymbol{\xi}_N = \boldsymbol{\gamma}_N^E + \boldsymbol{\epsilon}_N \boldsymbol{\gamma}_N^A \quad \boldsymbol{\xi}_T = \boldsymbol{\gamma}_T^E + \boldsymbol{\epsilon}_T \boldsymbol{\gamma}_T^A
\end{array} \tag{18}$$

The third line in (18) is used to compute $(\boldsymbol{\gamma}_N^A, \boldsymbol{\gamma}_T^A)$ from the known velocities \mathbf{u}^A at the left endpoint of the time interval and is thus no longer needed. The unknowns $(\boldsymbol{\gamma}_N^E, \boldsymbol{\gamma}_T^E)$

in the fourth line may be immediately eliminated with the help of the second line. This results in the reduced set of equations

$$\mathbf{M}(\mathbf{u}^E - \mathbf{u}^A) - \mathbf{h} \Delta t - \mathbf{W}_N \boldsymbol{\Lambda}_N - \mathbf{W}_T \boldsymbol{\Lambda}_T = 0 \quad (19)$$

$$\boldsymbol{\xi}_N = \mathbf{W}_N^\top \mathbf{u}^E + (\hat{\mathbf{w}}_N + \boldsymbol{\epsilon}_N \boldsymbol{\gamma}_N^A) \quad (20)$$

$$\boldsymbol{\xi}_T = \mathbf{W}_T^\top \mathbf{u}^E + (\hat{\mathbf{w}}_T + \boldsymbol{\epsilon}_T \boldsymbol{\gamma}_T^A) \quad (21)$$

which will be used in the sequel to set up the linear complementarity problem.

We are now going to formulate the inclusions from the last line in (17) as complementarity conditions. For the unilateral primitives we obtain by (2)

$$-\Lambda_{Ni} \in \text{Up}(\xi_{Ni}) \quad (i \in \mathcal{H}) \quad \Leftrightarrow \quad \boldsymbol{\Lambda}_N \geq 0, \boldsymbol{\xi}_N \geq 0, \boldsymbol{\Lambda}_N^\top \boldsymbol{\xi}_N = 0. \quad (22)$$

The relay functions have to be decomposed according to (5), but with a modified step height $[-\mu_i \Lambda_{Ni}, +\mu_i \Lambda_{Ni}]$ which gives

$$\begin{aligned} -\Lambda_{Ti} \in \mu_i \Lambda_{Ni} \text{Sgn}(\xi_{Ti}) \quad (i \in \mathcal{H}) \quad \Leftrightarrow \\ \exists \boldsymbol{\xi}_R, \boldsymbol{\xi}_L \in \mathbb{R}^k \text{ such that } \begin{cases} \boldsymbol{\mu} \boldsymbol{\Lambda}_N + \boldsymbol{\Lambda}_T \geq 0, \boldsymbol{\xi}_R \geq 0, (\boldsymbol{\mu} \boldsymbol{\Lambda}_N + \boldsymbol{\Lambda}_T)^\top \boldsymbol{\xi}_R = 0 \\ \boldsymbol{\mu} \boldsymbol{\Lambda}_N - \boldsymbol{\Lambda}_T \geq 0, \boldsymbol{\xi}_L \geq 0, (\boldsymbol{\mu} \boldsymbol{\Lambda}_N - \boldsymbol{\Lambda}_T)^\top \boldsymbol{\xi}_L = 0 \\ \boldsymbol{\xi}_T = \boldsymbol{\xi}_R - \boldsymbol{\xi}_L \end{cases} \quad (23) \end{aligned}$$

We further introduce $\boldsymbol{\Lambda}_R, \boldsymbol{\Lambda}_L \in \mathbb{R}^k$ to abbreviate the complementarity conditions in (23). They are defined, together with the last equation in (23), as

$$\boldsymbol{\Lambda}_R := \boldsymbol{\mu} \boldsymbol{\Lambda}_N + \boldsymbol{\Lambda}_T \quad (24)$$

$$\boldsymbol{\Lambda}_L := \boldsymbol{\mu} \boldsymbol{\Lambda}_N - \boldsymbol{\Lambda}_T \quad (25)$$

$$\boldsymbol{\xi}_T = \boldsymbol{\xi}_R - \boldsymbol{\xi}_L \quad (26)$$

The whole set of complementarity conditions (22), (23) therefore reads

$$0 \leq \begin{pmatrix} \boldsymbol{\xi}_N \\ \boldsymbol{\xi}_R \\ \boldsymbol{\Lambda}_L \end{pmatrix} \perp \begin{pmatrix} \boldsymbol{\Lambda}_N \\ \boldsymbol{\Lambda}_R \\ \boldsymbol{\xi}_L \end{pmatrix} \geq 0. \quad (27)$$

Note the special arrangement of $\boldsymbol{\Lambda}_L$ and $\boldsymbol{\xi}_L$. They must be placed in this manner, which has deep roots in optimization theory. Otherwise, one is not able to set up the LCP without additional matrix inversion processes.

By (27) we have already found the final description of the complementarity conditions of our problem, which also defines the vectors of variables that are allowed to be used. In addition, we still have equations (19)–(21) and (24)–(26) with the unknowns $\boldsymbol{\Lambda}_{N,R,L,T}$, $\boldsymbol{\xi}_{N,R,L,T}$ and \mathbf{u}^E . The magnitudes $\boldsymbol{\xi}_T$, Λ_T and \mathbf{u}^E have to be eliminated from this set of six equations, because they are not contained as variables in (27). In a first step, we use

(24) and (26) to remove Λ_T and ξ_T from the remaining equations. This yields for (19), (20), (21), (25)

$$\mathbf{M}(\mathbf{u}^E - \mathbf{u}^A) - \mathbf{h} \Delta t - (\mathbf{W}_N - \mathbf{W}_T \boldsymbol{\mu}) \Lambda_N - \mathbf{W}_T \Lambda_R = 0 \quad (28)$$

$$\xi_N = \mathbf{W}_N^T \mathbf{u}^E + (\hat{\mathbf{w}}_N + \epsilon_N \boldsymbol{\gamma}_N^A) \quad (29)$$

$$\xi_R = \mathbf{W}_T^T \mathbf{u}^E + (\hat{\mathbf{w}}_T + \epsilon_T \boldsymbol{\gamma}_T^A) + \xi_L \quad (30)$$

$$\Lambda_L = 2 \boldsymbol{\mu} \Lambda_N - \Lambda_R \quad (31)$$

In a second step, we solve (28) for \mathbf{u}^E which is always possible due to the regularity of the mass matrix \mathbf{M} ,

$$\mathbf{u}^E = \mathbf{M}^{-1}(\mathbf{W}_N - \mathbf{W}_T \boldsymbol{\mu}) \Lambda_N + \mathbf{M}^{-1} \mathbf{W}_T \Lambda_R + \mathbf{M}^{-1} \mathbf{h} \Delta t + \mathbf{u}^A, \quad (32)$$

and plug it in (29) and (30). As a result, we obtain (29)–(31) in matrix notation,

$$\begin{pmatrix} \xi_N \\ \xi_R \\ \Lambda_L \end{pmatrix} = \begin{pmatrix} \mathbf{W}_N^T \mathbf{M}^{-1} (\mathbf{W}_N - \mathbf{W}_T \boldsymbol{\mu}) & \mathbf{W}_N^T \mathbf{M}^{-1} \mathbf{W}_T & 0 \\ \mathbf{W}_T^T \mathbf{M}^{-1} (\mathbf{W}_N - \mathbf{W}_T \boldsymbol{\mu}) & \mathbf{W}_T^T \mathbf{M}^{-1} \mathbf{W}_T & \mathbf{E} \\ 2 \boldsymbol{\mu} & -\mathbf{E} & 0 \end{pmatrix} \begin{pmatrix} \Lambda_N \\ \Lambda_R \\ \xi_L \end{pmatrix} + \begin{pmatrix} \mathbf{W}_N^T \mathbf{M}^{-1} \mathbf{h} \Delta t + (\mathbf{E} + \epsilon_N) \boldsymbol{\gamma}_N^A \\ \mathbf{W}_T^T \mathbf{M}^{-1} \mathbf{h} \Delta t + (\mathbf{E} + \epsilon_T) \boldsymbol{\gamma}_T^A \\ 0 \end{pmatrix}, \quad (33)$$

where we have used the third line in (18) to express $(\mathbf{W}_N^T \mathbf{u}^A, \mathbf{W}_T^T \mathbf{u}^A)$ in terms of $(\boldsymbol{\gamma}_N^A, \boldsymbol{\gamma}_T^A)$. Equation (33) together with (27) is now the desired LCP $\mathbf{y} = \mathbf{A} \mathbf{x} + \mathbf{b}$, $0 \leq \mathbf{y} \perp \mathbf{x} \geq 0$ of dimension $3k$.

Note the following properties of the LCP (33), (27): For friction that is independent of the normal load Λ_{Ni} , the terms $\mu_i \Lambda_{Ni}$ have to be replaced by constants a_i and move into the vector \mathbf{b} of the LCP. The resulting matrix \mathbf{A} is then bisymmetric, and the LCP states the Kuhn-Tucker conditions of an associated quadratic program with inequality constraints, see [2]. For $\Delta t = 0$, the LCP reduces to the pure impact equations and can be used, for example, for initialization of the velocities. For $\boldsymbol{\gamma}_N^A = \boldsymbol{\gamma}_T^A = 0$, the LCP describes impact-free motion on velocity level, containing still the cases of persisting contact and stiction as well as transitions to sliding or separation, and can be transformed to the acceleration level by the methods shown in [2].

References

- [1] Glocker, Ch.: Dynamics of Structure-Variant Systems. Graduate lecture for mechanical engineers at ETH Zurich.
- [2] Glocker, Ch.: Set-Valued Force Laws: Dynamics of Non-Smooth Systems. Springer Verlag, Berlin, Heidelberg 2001.

- [3] Leine, R.I., Glocker, Ch., van Campen, D.H.: Nonlinear Dynamics and Modeling of Various Wooden Toys with Impact and Friction. *Journal of Vibration and Control* **9**, pp. 25–78, 2003.
- [4] Moreau, J.J.: Unilateral Contact and Dry Friction in Finite Freedom Dynamics, in: *Non-Smooth Mechanics and Applications* (Eds. J.J. Moreau, P.D. Panagiotopoulos), CISM Courses and Lectures Vol. 302, 1–82, Springer Verlag, Wien 1988.
- [5] Pfeiffer, F., Glocker, Ch.: *Multibody Dynamics with Unilateral Contacts*. John Wiley & Sons, New York 1996.